

IMPACT OF GEOMETRY ON ELEMENT ABUNDANCES FROM X-RAY FLUORESCENCE IN VACUUM: CONSIDERATIONS FOR APXS MEASUREMENTS ON SMALL AIRLESS BODIES.

J. I. Núñez¹, E. Y. Adams¹, L. J. Koerner¹, S. L. Murchie¹, ¹Johns Hopkins University Applied Physics Laboratory (11100 Johns Hopkins Road, Laurel, MD 20723; jorge.nunez@jhuapl.edu)

Introduction: Over the past two decades, the Alpha Particle X-ray Spectrometer (APXS) instruments onboard Mars Pathfinder (MPF) [1], the Mars Exploration Rovers (MER) Spirit and Opportunity [2-5], and more recently the Mars Science Laboratory (MSL) Curiosity [6-8] have successfully measured the bulk chemical composition of rocks and soils *in situ* on the Martian surface by x-ray spectroscopy. The APXS instruments employ Curium-244 sources that generate alpha particles and x-rays to irradiate the surface materials and measure the emitted x-ray spectra using silicon drift detectors. The emitted x-ray spectra have peaks at energies that are characteristic of different elements. This enables the instruments to provide abundances of elements ranging from sodium (Na; Z = 11) up to bromine (Br; Z = 35) as in the case of the MER APXS [5].

The ESA Rosetta mission to comet 67P/Churyumov-Gerasimenko also includes an APXS instrument as part of the instrument payload on the Lander “Philae” that will land on the comet nucleus [9-10]. Similar to the MER APXS, the Rosetta APXS will measure the abundance of elements ranging from sodium (Na; Z = 11) up to nickel (Ni; Z = 28) of the surface of the comet nucleus at the Philae landing site [9]. While the MER and MSL APXS instruments are deployed on a robotic arm that positions the sensor head to within a few mm from the target surface, the Rosetta APXS will be positioned using a deployment device that lowers the sensor head to the comet’s surface [9].

Measurements of element abundances using x-ray spectroscopy and derived element ratios are dependent on instrument position and orientation from the target surface. While past missions have utilized mechanical instrument deployment devices (IDDs) such as a robotic arm to properly position instruments like APXS to the target surface, future small landers to asteroids and comets, such as the Planetary Object Geophysical Observer (POGO) [11] or the Mobile Asteroid Surface Scout (MASCOT) lander [12] on the JAXA Hayabusa 2 mission to NEO C-type asteroid 1999 JU3 [13], may not employ IDD to be able to properly position instruments to the target surface. This poses a potential challenge for obtaining proper APXS measurements of element abundances on small bodies as the APXS instrument may not be properly positioned due to the instrument being at a large standoff distance or large tilt angle from nadir from the target surface.

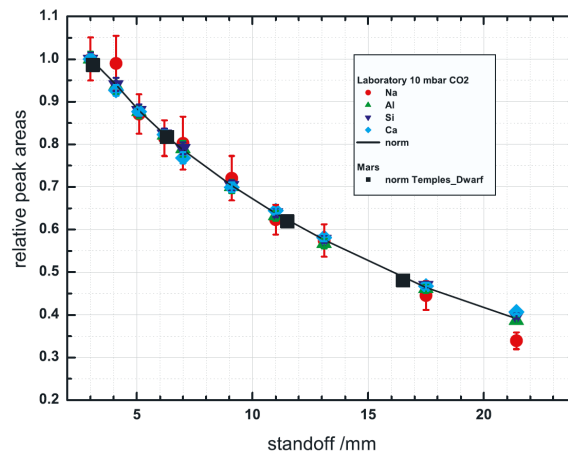


Figure 1. Laboratory measurements of element abundance ratios of the calibration sample SSK at different standoff distances under 10 mbar CO₂ environment relative to 2 mm distance from contact ring to sample surface (Figure from [5]).

Past work with MPF and MER APXS instruments in the laboratory and on Mars have shown that while APXS signal is attenuated with increasing standoff distance from the target surface (up to 20 mm) due to the martian atmosphere, measurements of element abundances and derived element ratios are not significantly impacted (Figures 1 and 2) [1; 5]. Recent work with MSL [7] and Chandrayaan-2 [14-15] APXS instruments show that even larger standoff distances (up to ~90 mm) also do not impact element abundance measurements. Under vacuum, this standoff distance could be increased as the lack of an atmosphere provides less attenuation of alphas and x-rays. Thus, the Chandrayaan-2 APXS will operate from ~180 mm from the lunar surface [15]. Since little work has been done on the impact of angle position on APXS measurements, here we present work to assess the impact of angle tilt on measurements of element abundances and derived element ratios using an APXS under vacuum.

Instrument and Measurements: We used an APXS prototype instrument developed at APL that includes a PX5 supply and processing unit, FW6 DPP MCA control software, and XR-100SDD x-ray detector system. The XR-100SDD system includes a silicon drift detector (SDD) with 25 mm² active area. The SDD has a low-energy ‘C2’ window (aluminized silicon-nitride) with transmission of 41.9% at the carbon K α line (277 eV).

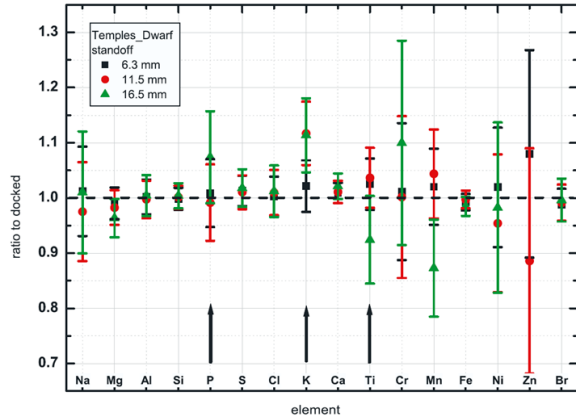


Figure 2. APXS measurements of element abundance ratios at different standoff distances up to 16.5 mm relative to 3.1 mm distance from the contact ring of the rock dubbed “Temples Dwarf” in the Columbia Hills in Gusev crater by the MER rover Spirit (Figure from [5]). The element ratios fall within measurement error bars. The black arrows correspond to elements affected by background signals (See [5] for more details).

We used an Americium-241 radioactive source with activity of 540 μCi due to the limited availability of Curium-244 sources. Americium-241 produces alpha particles of 5.486 MeV and x-rays of 60 keV, while Curium-244 produces 5.805 MeV alphas and x-rays with energy of 14 keV and 18 keV [2].

The x-ray spectrum is divided into 2048 channels resulting in an energy resolution of 130 eV at 5.9 keV at a detector temperature of 224K. This is an improvement in energy resolution compared to the 160 eV resolution at 5.9 keV for the MER APXS instruments [2].

The instrument and sample were placed in a light-tight aluminum vacuum chamber with a vacuum of $3.6\text{E}-2$ Torr. The detector was tilted at different angles (φ) from perpendicular to the sample surface (i.e., $\varphi = 0^\circ$ detector tilt) to assess the impact of detector tilt on element abundance measurements (Figure 3). Measurements were collected over ~ 20 hour integrations.

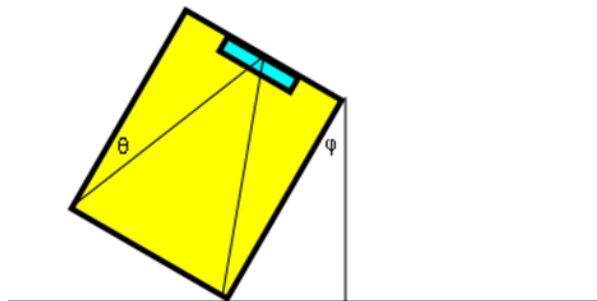


Figure 3. Diagram showing detector tilt from perpendicular to the target surface (φ).

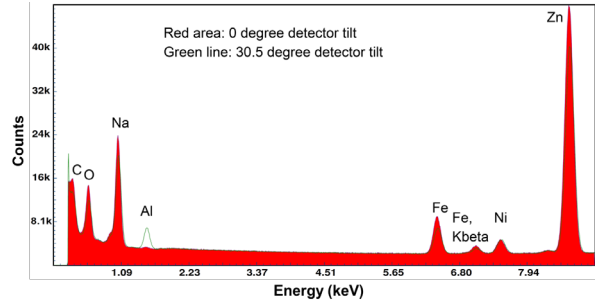


Figure 4. X-ray spectrum of calibration target in vacuum at 0° (red area) and 30.5° (green line) detector tilt from perpendicular to target surface. The Al peak in the green line corresponds to the detector seeing part of the wall of the aluminum vacuum chamber. The peak areas are used to calculate abundance ratios (Figure 5).

Results: Figures 4 shows the X-ray spectrum of a calibration target (composed of 50% galvanized stainless steel and 50% kapton tape) measured with the prototype APXS instrument under vacuum at 0° and 30.5° detector tilt from perpendicular to the sample surface.

Figure 5 shows the element abundance ratios of the corresponding elements shown in Figure 4 along with their respective measurement error bars. Analysis of the peak areas in Figure 4 shows a drop in the peaks for all elements (except Al) for the 30.5° tilt compared to the 0° tilt, consistent with a drop of the x-ray signal due to the offset angle. However, despite the drop in x-ray signal for each element, the relative abundance of each element with respect to the total amount remains the same as shown in Figure 5, where the relative abundance of each element at 30.5° tilt is ratioed to the relative abundance of each element at 0° . In this case the ratio for each element is close to 1, with those that are offset by a greater amount falling within measurement error bars. Thus a detector angle of up to $\sim 30^\circ$ does not appear to significantly impact element abundances.

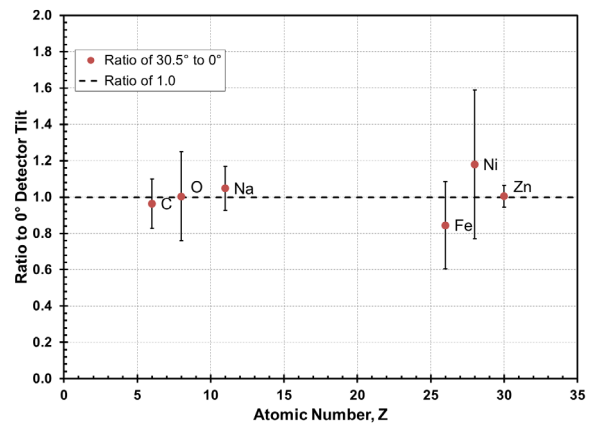


Figure 5. Element abundance ratios at 30.5° detector tilt relative to 0° detector tilt of calibration target from

Figure 4 measured using prototype APXS instrument. The element ratios fall within measurement error bars. The element ratio for aluminum (Al) is not included in the plot due to the detector seeing part of the wall of the aluminum vacuum chamber.

This is also the case over different angles as well as ratios of different elements. In Figure 6, the x-ray signal for each elements drops considerably with increasing angle tilt (as shown in panels A and B). However, the slope in the drop in signal for each element is predominantly linear with increasing angle tilt up to 30°. This enables element abundance ratios to remain roughly the same regardless of tilt (as shown in panel C). Beyond 30° tilt, the element slopes deviate with larger changes seen in the heavier elements compared to the lighter elements. This results in greater abundance errors when calculating abundance ratios at higher angles. However, these errors remain relatively low (~1-2% error) at up to 45° tilt.

Discussion and Summary: The Hayabusa mission to the near-Earth asteroid (NEA) 25143 Itokawa revealed that Itokawa was a gravitationally accumulated, rubble pile [16] with significant surface roughness [17]. A small lander like POGO or MASCOT deployed on such surface would most likely result in contact instruments like an APXS not being properly positioned on the regolith surface. This work along with past work by [5-7; 14-15] show that tilt angles as high as ~45° and standoff distances up to ~180 mm will not significantly impact element abundance measurements

with an APXS under vacuum conditions. Thus, an APXS instrument deployed on a small lander would be capable of measuring abundances of major and key minor elements present on an asteroid or comet surface, even if it is not properly positioned, due to the lack of an atmosphere on the small body to attenuate the alpha and x-ray signal. This expands the utility of an APXS instrument to properly measure the abundance of elements from small airless bodies.

References: [1] Rieder R. et al. (1997) *Science*, 278, 1771-1774. [2] Rieder R. et al. (2003) *J. Geophys. Res.*, 108, 8066, doi:10.1029/2003JE002150. [3] Rieder R. et al. (2004) *Science*, 306, 1746-1749. [4] Gellert R. et al. (2004) *Science*, 305, 829-832. [5] Gellert R. et al (2006) *J. Geophys. Res.*, 111, doi:10.1029/2005JE002555. [6] Campbell et al. (2012) *Space Sci. Rev.*, 170, 319-340. [7] Gellert R. et al. (2013) *LPS XLIV*, Abstract #1432. [8] McLennan S. et al. (2014) *Science*, 343, 1244734, doi:10.1126/science.1244734. [9] Bibring J.-P. et al. (2007) *Space Sci. Rev.*, 128, 205-220. [10] Klingelhöfer G. (2007) *Space Sci. Rev.*, 128, 383-396. [11] Hill S. W. et al. (2014) *2nd IWIPM*, this meeting. [12] Jaumann R. et al. (2013) *LPS XLIV*, Abstract #1500. [13] Tsuda Y. et al. (2013) *Acta Astronautica*, 91, 356-362. [14] Goyal S. K. et al. (2013) *IEEE NSS/MIC*, doi:10.1109/NSSMIC.2013.6829708. [15] Shanmugam M. et al. (2013) *Adv. Space Res.*, doi:10.1016/j.asr.2013.03.011. [16] Fujiwara et al. (2006) *Science*, 312, 1330-1334. [17] Barnouin et al. (2008) *LPS XXXIX*, Abstract #1297.

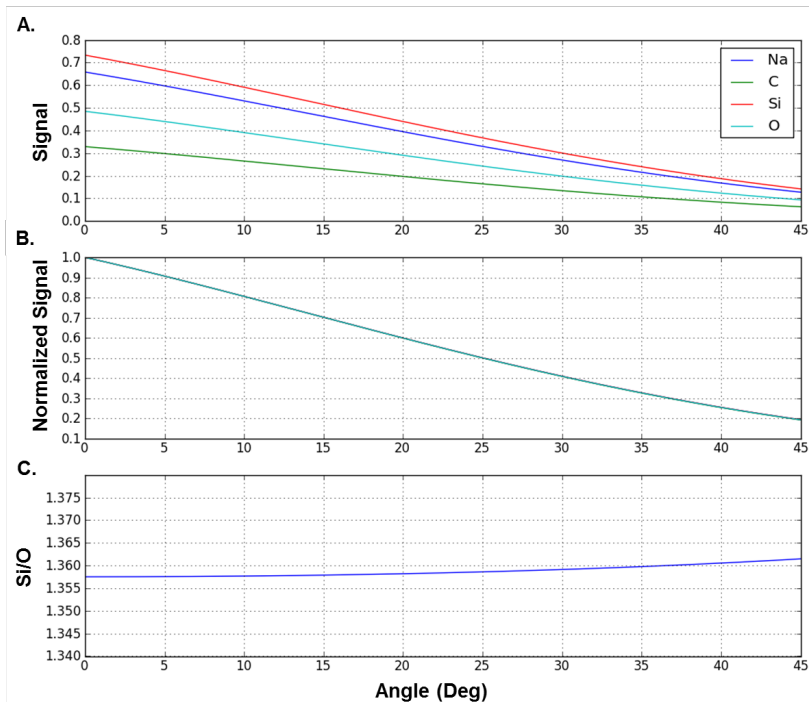


Figure 6. Element abundances (A), normalized signal (B), and derived example Si/O ratio (C) relative to detector angle tilt as shown in Figure 3. Plots show that x-ray signal is attenuated with increasing detector tilt from perpendicular to target surface. Angles of less than 30° do not significantly impact element abundance ratios.